Return Intervals Approach to Financial Fluctuations

Fengzhong Wang[1], Kazuko Yamasaki[1,2], Shlomo Havlin[1,3], and H. Eugene Stanley[1]

[1] Center for Polymer Studies and Department of Physics, Boston University, Boston, MA 02215, USA
[2] Department of Environmental Sciences, Tokyo University of Information Sciences, Chiba 265-8501, Japan
[3] Minerva Center and Department of Physics, Bar-Ilan University, Ramat-Gan 52900, Israel

Abstract. Financial fluctuations play a key role for financial markets studies. A new approach focusing on properties of return intervals can help to get better understanding of the fluctuations. A return interval is defined as the time between two successive volatilities above a given threshold. We review recent studies and analyze the 1000 most traded stocks in the US stock markets. We find that the distribution of the return intervals has a well approximated scaling over a wide range of thresholds. The scaling is also valid for various time windows from one minute up to one trading day. Moreover, these results are universal for stocks of different countries, commodities, interest rates as well as currencies. Further analysis shows some systematic deviations from a scaling law, which are due to the nonlinear correlations in the volatility sequence. We also examine the memory in return intervals for different time scales, which are related to the long-term correlations in the volatility. Furthermore, we test two popular models, FIGARCH and fractional Brownian motion (fBm). Both models can catch the memory effect but only fBm shows a good scaling in the return interval distribution.

Keywords: Financial marekts, Econophysics, Volatility, Return interval, Scaling, Long-term correlation.

1 Introduction

Large and unpredictable fluctuations constitute risk for investments as well as the whole economy. For instance, the credit crisis nowadays is along with turmoil in financial markets, which causes huge losses for many investors and likely initiates a recession worldwide. Moreover, significant risk could be inherent not only in market crashes, but also in less hazardous fluctuations if they are unexpected and investments are not well protected against them. Banks have to properly estimate the risk of their investments and make provisions in order to be able to withstand large fluctuations without going bankrupt. The importance of financial markets attract many researchers and in particular, collaborative work

J. Zhou (Ed.): Complex 2009, Part I, LNICST 4, pp. 3–27, 2009.

joining economists and physicists (which created a new interdisciplinary field of econophysics [1,2,3,4,5,6,7,8,9,10,11,12,13,14,15,16,17,18,20,19,21,22,23,24,25] [26,27,28,29,30,31,32,33,34,35]) has resulted in a better understanding of economic fluctuations. Until relatively recently, theories of economic fluctuations invoked the label of "outliers" (bubbles and crashes) to describe fluctuations that do not agree with the existing theory. However, econophysics research found evidence that the probability distribution of price fluctuations can be described by a power law [27,28,29,30,31,32,33,34,35]. There are no "outliers" since this law also holds for extremely large and unpredictable changes of magnitude sufficient to wreak havoc.

Statistical physics deals with systems comprising a very large number of interacting subunits, for which predicting the exact behavior of the individual subunit would be impossible. Hence, one is limited to making statistical predictions regarding the collective behavior of the subunits. Recently, it has come to be appreciated that many such systems consisting of a large number of interacting subunits obey universal laws, therefore they are independent of the microscopic details. The finding, in physical systems, of universal properties that do not depend on the specific form of the interactions gives rise to the intriguing hypothesis that universal laws or behavior may also be present in economic and social systems [34,35]. An often-expressed concern regarding the application of physics methods to the social sciences is that physical laws are applied to systems with a very large number of subunits (at the order of Avogadro's number, 10^{23}), while social systems comprise a much smaller number of elements. Fortunately, due to the rapid development of electronic trading and data storing in the last few decades, financial data bases have become available with a huge amount of data points (say 10^8), enabling physicists to analyze them as dynamic systems. The data size becomes comparable to nano systems and the "thermodynamic limit" is reached so that methods from statistical physics can be applied. It is worth to note that there is only a small amount of extremely large events even in very huge data bases. To understand these devastating events, it is of great importance to find laws describing the entire data set in order to approach extreme events by extensive analysis on small fluctuations.

Two important conceptual advances on universal laws are *scaling* and *universality*. A system obeys a scaling law if its relation is characterized by the same functional form and exponent over a certain range of scales ("scale invariance"). The typical behavior for scaling is *data collapse*, all curves can be "collapsed" onto a single curve, after a certain scale transformation on the measure. The general principles of scale invariance used here have proved useful in interpreting a number of other phenomena, ranging from elementary particle physics and galaxy structure to finance [35,36,37]. At one time, many imagined that the "scale-free" phenomena are relevant to only a fairly narrow slice of physical phenomena [38,39]. However, the range of systems that apparently display power law and scale-invariant correlations has increased dramatically in recent years, ranging from base pair correlations in noncoding DNA [40], lung inflation [41] and interbeat intervals of the human heart [42] to complex systems involving

large numbers of interacting subunits that display "free will," such as city growth [43], university research budgets [44], and even bird populations [45]. In many of these diverse systems, the *same* scaling function exists for a significant range which is remarkable, apparently suggesting the universality of laws. Moreover, many systems share the same scaling functions and characteristic exponents and therefore belong to one universality class. This connection provides the people a comprehensive view over these diverse systems.

Scaling and universality are important properties of a data set describing the global behavior of the probability distribution. This usually does not fully characterize a sequence of data points which also depends on the time organization of the sequence. Only if it is *uncorrelated*, the data points are independent of each other and the sequence is totally determined by the distribution. In most cases, the records is *correlated*, it will affect the order in the data set. This behavior is called "memory", as the data points "remember" previous values. Trivially the memory decays with the time lag. The decay of memory, which could be characterized by the autocorrelation function, may follows different types of function. One typical function is exponential, and the existing of memory is described by a characteristic time scale. The memory almost disappears at the scales above the characteristic time and thus it only exists for a short-term. Such kind of time series is called *short-term correlated*. Another typical function for the autocorrelation is a power law. In this case there is no finite characteristic scale and the correlation exists for a much longer time, therefore it is called *long-term correlated*. Note that short-term memory always exists in a long-term correlated time series. As for the study of financial markets, the temporal structure in a time series is of great importance since it influences the performance of any movement. Many studies show that price change ("return") does not exhibit any linear correlations extending over more than a couple of minutes, but their absolute value, which is a measure of volatility, exhibits long-term correlations (see Ref [34] and references therein). This leads to long periods of high volatility as well as other periods where the volatility is low ("volatility clustering").

Extreme events do not only occur in economics, but also appear in very different fields like climate or earthquakes. For instance, Gutenberg and Richter related huge earthquakes to everyday tremors in one single power law curve [46,47]. If one wants to prepare for a dangerous earthquake, it might be less important to exactly know how strong the next shock will be, but rather to know when a large shock will occur. A good approach is to study the time ("return interval") between two successive shocks larger than a threshold above which a shock would damage a building. This way one can gather information on the temporal structure of the fluctuations. Recently Bunde et al. [48,49,50,51] studied the return intervals for climate records and found that the long-term memory leads to a stretched exponential distribution and clustering of extreme events. They also suggested that these phenomena should therefore also occur in heartbeat records, internet traffic and stock volatility where long-term correlations occur. For financial data, a first effort was conducted by Yamasaki et al. who studied the daily data of currencies and US stocks and showed the scaling in the

distribution and long-term memory in the sequence [52]. Following this, Wang et al. studied the intraday data of 30 stocks which constitute of Dow Jones Industrial Average (DJIA) index, Standard and Poor's 500 (S&P 500) index, currencies, interest rates as well as oil and gold commodities and found similar behaviors [53,54]. Similar analysis have been done for the Japanese [55] and Chinese [56,57] stock markets. To compare with the empirical data, Vodenska-Chitkushev et al. examined return intervals from two known models, FIGARCH and fractional Brownian motion (fBm) and showed that both models simulate the memory effects but only fBm yield the scaling feature [58]. Bogachev et al. related the nonlinear correlations to the multiscaling behavior in return intervals [59], they also showed that the return interval distribution follows a power law function for multifractal data sets [63]. Recently, Wang et al. studied systematically 500 components of S&P 500 index and demonstrated a systematic deviation from the scaling. They showed that this multiscaling behavior is related to the nonlinear correlations in volatility sequence [60]. Further, Wang et al. analyzed the relation between multiscaling and several essential factors, such as capitalization and number of trades, and found certain systematic dependence [61]. The multiscaling behavior is also found in the Chinese stock market [62]. These studies help us to better understand the volatility and therefore may lead to better risk estimation and portfolio management [64,65,66,67]. Return

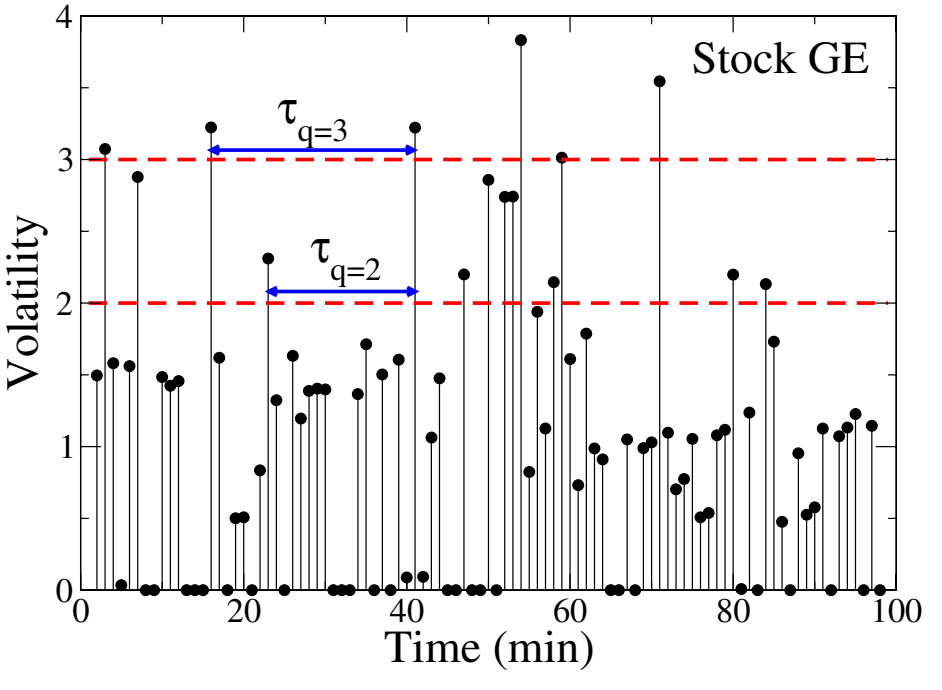

Fig. 1. (Color online) Illustration of volatility return intervals. The volatility is in units of its standard deviation. The solid circles are volatility values of the GE stock on Jan 8, 2001. Return intervals $\tau_{q=2}$ and $\tau_{q=3}$ for two typical thresholds q are displayed.

intervals have also been studied in many other fields (see Ref [68] and references therein). It is calculated in similar ways but with different names, like waiting time, interocurrence time or interspike interval.

In this paper we analyze the volatility return intervals of the entire US stock markets. The database analyzed is the Trades And Quotes (TAQ) from New York Stock Exchange (NYSE). The period studied is from Jan 2, 2001 to Dec 31, 2002, totally 500 trading days. TAQ records every trade for all securities in the US markets. To avoid many missing points in 1-min resolution, we choose to analyze only the 1000 most traded stocks. Their numbers of trades range from 600 to 60,000 times per day. The volatility is defined the same as in Ref [53]. First, we compute the absolute value of the logarithmic change of the minute price, then remove the intraday U-shape pattern, and finally normalize the series with its standard deviation. Therefore the volatility is in units of standard deviations. With 1-min sampling interval, a trading day has 390 points (after removing the market closing hours), and each stock has about 195,000 records. We also examine the S&P 500 index, a benchmark of US stock markets. The data is from Jan 2, 1984 to Dec 31, 1996, totally 130,000 points with 10-min sampling interval. For a typical stock, General Electric (GE), we find volatilities above a certain threshold q and calculate time intervals between them, as illustrated in Fig. 1. These time intervals consist the return interval series and the only free parameter is the threshold q.

2 Distribution of Return Intervals

We begin by analyzing the distribution, one of most important statistical properties for a time series. The distribution can be characterized by probability density function (PDF) or cumulative distribution function (CDF). Previous studies [52,53,54,55,56,57,58,59,60,61,62] showed that PDF for the return interval τ, $P(\tau)$, can be well approximated by a scaling law if τ is scaled by its average $\langle\tau\rangle$ ($\langle ...\rangle$ stands for the average over a data set), i.e.,

$$P(\tau) = 1/\langle\tau\rangle \cdot f(\tau/\langle\tau\rangle). \tag{1}$$

The scaling function f does not depend explicitly on q, but only through the mean interval $\langle\tau\rangle$. If $P(\tau)$ is known for one value of q, Eq. (1) can make predictions for other values of q—in particular for very large q (extreme events), which are difficult to study due to the lack of statistics.

2.1 Stretched Exponential Distribution

An important question is, what is the form of scaling function f? For many markets, the function was suggested to be in a good approximation to a stretched exponential (SE) [52,53,54,55,56,57,58,59,60,61,62],

$$f(x) \sim e^{-(x/x^*)^\gamma}. \tag{2}$$

Here x^* is the characteristic scale and γ is the shape parameter, which is related to the correlations in the volatility sequence and thus called "correlation exponent" [49]. For an uncorrelated series, f reduces to the regular exponential function and $\gamma = 1$. From Eq. (2), the PDF function can be rewritten as

$$P(\tau) \sim e^{-(\tau/a)^\gamma}. \tag{3}$$

Then a is the characteristic scale. From the definition of PDF and $\langle\tau\rangle$, one may find that the parameter a depends exclusively on γ [68,60],

$$a = \langle\tau\rangle \cdot \Gamma(1/\gamma)/\Gamma(2/\gamma). \tag{4}$$

Here $\Gamma(a) \equiv \int_0^\infty t^{a-1}e^{-t}dt$ is the Gamma function. However, due to the discreteness and finite size effects, there are some systematic deviations from the scaling law [51,60]. To avoid them, we will also use a as a free parameter in the SE fit. To simplify the calculation and without loss of generality, we assume τ/a is continuous, then the corresponding CDF, $C(\tau)$, is the integral of the PDF,

$$C(\tau) \equiv \int_x^\infty P(\tau)d\tau \sim \Gamma(1/\gamma, (\tau/a)^\gamma). \tag{5}$$

where $\Gamma(a, x) \equiv \int_x^\infty t^{a-1}e^{-t}dt$ is the incomplete Gamma function. Since CDF accumulates the information of the series and has a better statistics than PDF, in the following we obtain the correlation exponent γ by fitting the CDF with Eq. (5).

As an example, we plot three CDFs (for $q = 2$, 4 and 6 respectively) of the GE stock in Fig. 2. The three curves are distant from the other, due to the difference in $\langle\tau\rangle$. The least-square fits with Eq. (5) are illustrated by the solid lines. We use the classical method, Kolmogorov-Smirnov (KS) Statistic D, to test the goodness-of-fit [69,70]. D is defined as the maximum absolute difference between the cumulative distribution of the original data $C(\tau)$ and that of the fit $F(\tau)$,.

$$D \equiv max(|C(\tau) - F(\tau)|). \tag{6}$$

When D is larger than a certain value, which is called critical value (CV), the SE distribution is rejected. CV is decided by the significance level and data size. In this paper we choose 1% significance level and

$$CV = 1.63/\sqrt{N}, \tag{7}$$

where N is the number of data points.

We fit CDF with SE function for the 1000 most traded stocks [71]. The range of threshold is from $q = 1$ to 6, and the number of fit that is not rejected ("good fit") is listed in Table 1. We can see that most of the cases have a good fit by a SE function. A question naturally arises, for different thresholds, how similar are these correlation exponents? Previous research show that the scaling in distribution is well approximated [52,53,54,55,56,57,58,59,60,61,62]. Trivially, γ for different thresholds are strongly related, and their discrepancy should be

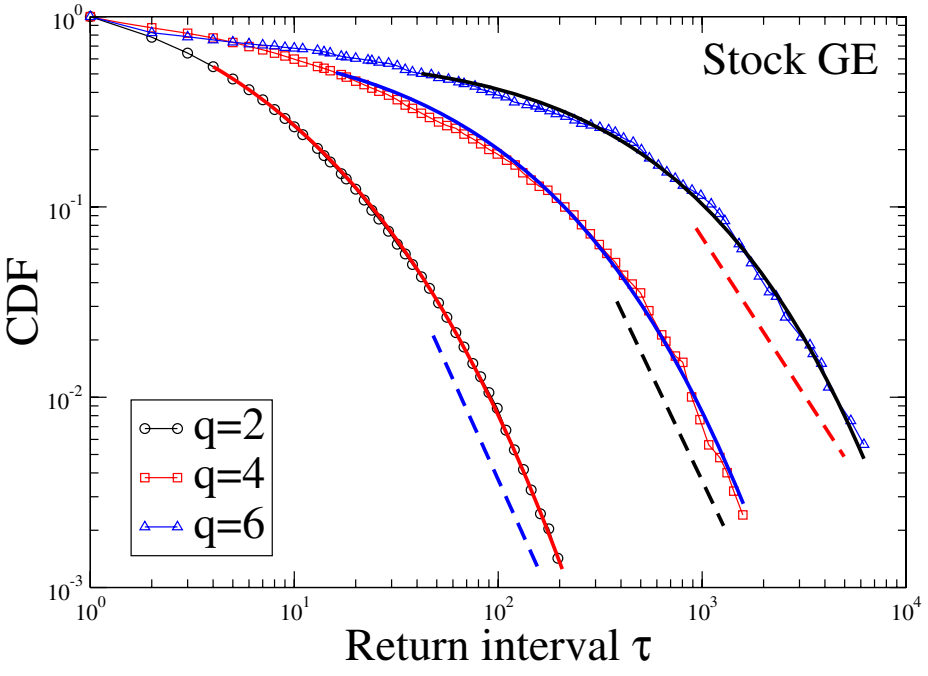

Fig. 2. (Color online) Cumulative distribution function (CDF) of return interval τ. CDF of three typical thresholds $q = 2$, 4 and 6 for the GE stock are plotted. Examples of two types of fit, the dashed lines (left shifted for better visibility) are the power law fit for the distribution tails and the solid lines on symbols are the stretched exponential fit for the whole distributions.

Table 1. Number of good fit on return interval CDF of the 1000 stocks. If KS statistics D (Eq. (6)) is smaller than the critical value CV (Eq. (7)), the corresponding distribution is not rejected. Two types of distribution, stretched exponential (for the whole range) and power law (for the tail), are tested.

Threshold q	1	2	3	4	5	6
Stretched exponential fit	791	795	815	933	977	986
Power law fit	31	349	626	826	839	710

small. To test this assumption we plot in Fig. 3 the dependence of the γ for other thresholds on the γ obtained for $q = 2$. Remarkably, all four cases show significant tendency and the slopes of linear fit are very close to 1. This result supports the well-approximated scaling in the distribution of return intervals. Note that the fluctuation is larger for a higher q, and the slope slightly decreases, which may be due to the limited data size of return intervals for large thresholds. We also test the dependence of other pairs of thresholds and observe similar behaviors. All these behaviors are consistent with Ref [61]. Moreover, we compare the value of the parameter a with Eq. (4) and find that a from the fit is in the same order

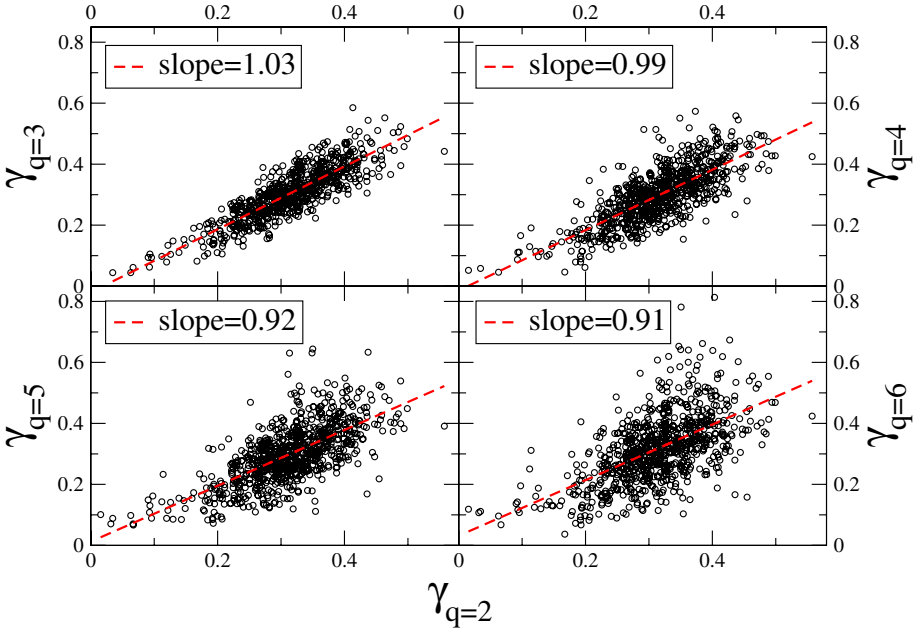

Fig. 3. (Color online) Relation between correlation exponent γ (Eq. (3)) of different thresholds. γ for four thresholds, $q = 3$ to 6 strongly depend on γ for $q = 2$, as indicated by dashed lines from the linear fit. All slopes of fit are quite close to 1, which suggests a good scaling in the distribution of return interval. Note that the fluctuation becomes stronger for a larger q, which relates to the smaller data size for the return interval with a larger q.

as that from Eq. (4), and usually the former is smaller. The ratio between two a is centered from 0.4 (for $q = 1$) to 0.8 (for $q = 6$) for the 1000 stocks [72].

2.2 Power Law Tail

For financial time series, the distribution tail usually is characterized by a power law function [27,28,29,30,31,32,33,34,35]. As for the return interval, Yamasaki et al. suggested that the scaling function is also consistent with a power law tail for large intervals, where the tail exponent is around 1 for both stock and currency data [52]. Moreover, Bogachev and Bunde have shown that the distributions of return intervals are governed by power laws [63]. Then CDF of return intervals would follow

$$C(\tau) \sim \tau^{-\zeta}, \tag{8}$$

where ζ is the tail exponent. To test this hypothesis we examine the distribution tail for the 1000 stocks. A popular way to fit the tail is using the Maximum Likelihood Estimator, specifically, it also called Hill estimator for a power law

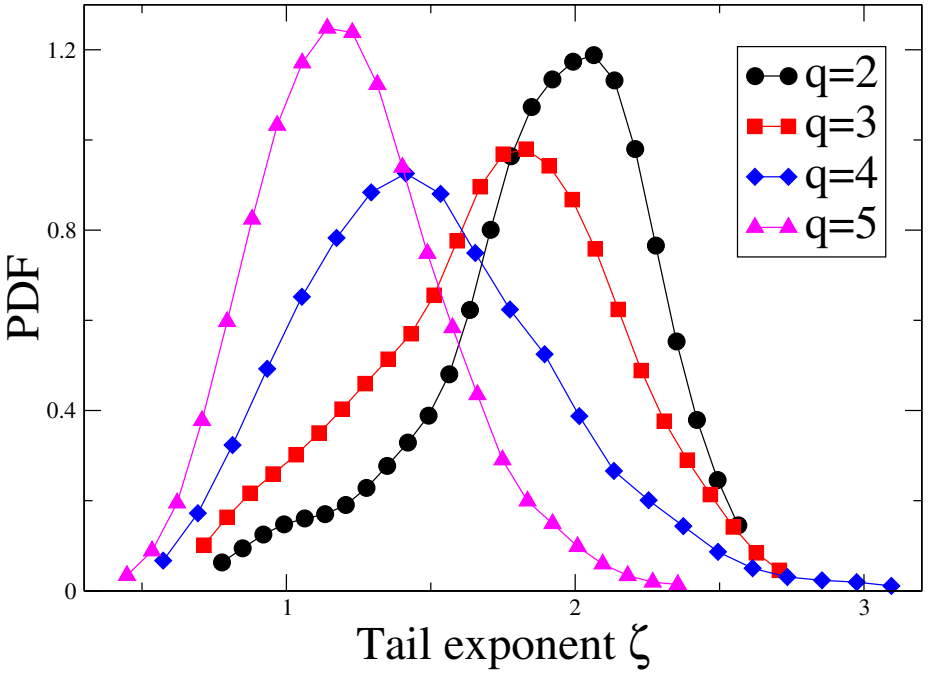

Fig. 4. (Color online) Probability density function (PDF) of tail exponent ζ from power law fit on the cumulative distribution of return intervals. The distribution systematically shifts from right to left, with increasing of the threshold.

tail [32,33,73]. The range of fit is not fixed by the Hill estimator [32,33], thus we examine the entire tail and choose the range that has the minimum KS statistics [33]. Examples of power law fits are demonstrated by the dashed lines in Fig. 2. We still use KS statistics to test the goodness-of-fit. For threshold $q = 1$ to 6, the numbers of good fit are listed in Table 1. For return intervals of $q = 1$ and 2, only for a small portion of the 1000 stocks, the power law distribution is not ruled out. However, for other cases, the power law distribution is not ruled out for a significant portion of stocks. In Fig. 4 we plot the PDF for tail exponent ζ. Interestingly, all PDFs are centered around a certain value which systematically shift from large value to small, with increasing the threshold. For $q = 2$, ζ is centered around 2, and for $q = 5$, ζ is centered around 1. The latter is consistent with Ref [52], which suggests that the difference may due to the limited size of data points. Ref [52] was using daily data, which is about 1/20 of the intraday data in the current paper ($\sim 10,000$ points for the daily data vs. $\sim 195,000$ points for the intraday data). Similarly, the number of return intervals for $q = 5$ is only about 1/14 of that for $q = 2$ (average over the 1000 stocks, ~ 850 points for $q = 5$ vs. $\sim 11,800$ points for $q = 2$). We also must note that, for $q = 2$, only about 1/3 of the 1000 stocks have a good power law fit (Table 1).

2.3 Universality of Scaling

Fig. 3 supports quite impressive the universality hypothesis of the correlation exponent γ since it holds for a broad market, the 1000 most traded stocks in the US markets, with a wide range of thresholds. Recent studies confirmed that the scaling is also valid for other important markets, such as the Japanese market, a typical mature market, and the Chinese market, a prominent emerging market. Jung et al. analyzed the intraday data for 1817 stocks (1 year) and daily data for 3 typical companies (28 years) from the Japanese market [55]. They showed similar results as that of the US markets. For the Chinese market, 2 indices and 30 liquid stocks (both 2.5 years) were investigated, their behavior is also consistent with the US markets [56,57,62]. Moreover, currencies [52,54], interest rates, oil and gold commodities [54] were also found to follow a scaling law. Remarkably, γ is centered between 0.3 and 0.4 for all cases as seen in Fig. 3 and the similar γ was found in other investigations [52,53,54,55,56,57,58,59,60,61,62]. To conclude, the scaling in return interval distribution is valid for two dimensions, different financial assets and different volatility thresholds.

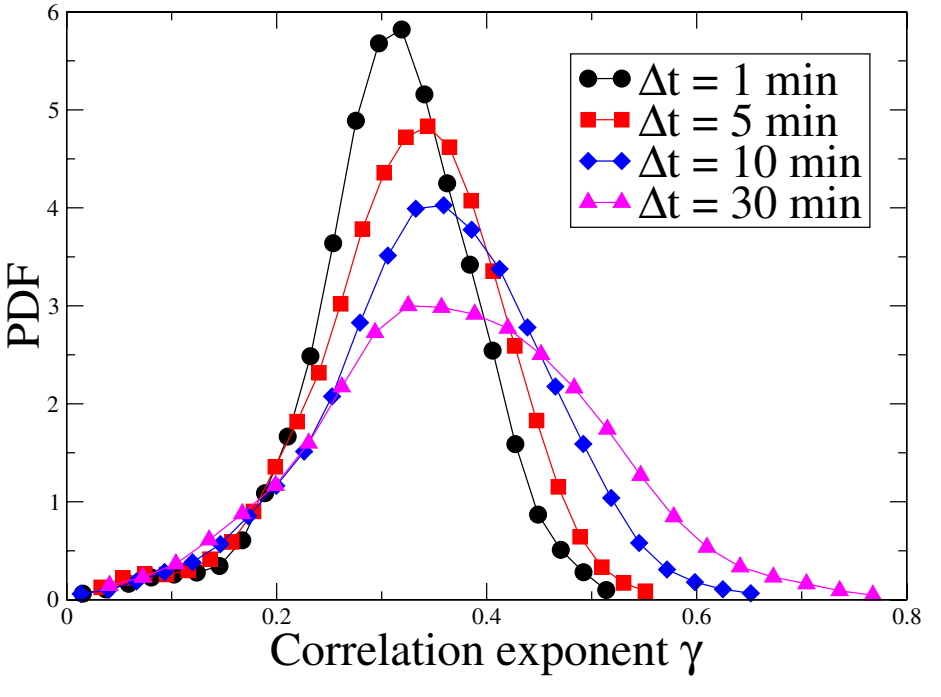

Fig. 5. (Color online) Distribution of correlation exponent γ for four sampling intervals, $\Delta t = 1$, 5, 10 and 30 minutes. With increasing of the sampling interval, the distribution tends to be wider. However, their centers are still close, changing from 0.31 for $\Delta t = 1$ minute to 0.37 for $\Delta t = 30$ minutes, which suggests that scaling is a good approximation for this range of sampling intervals. The broader distribution for lower resolution may be related to its smaller data size.

For statistical analysis, the time resolution of the records is an important aspect since the system may exhibit diverse behaviors in different time windows Δt. This is the third dimension for testing the universality of scaling. In Ref [54], Wang et al. have shown that the scaling is valid even to a sampling interval of 1 trading day. Here we change the volatility sampling interval from 1 minute to 5, 10 and 30 minutes, and then examine its return interval CDF. For 1-day resolution, there is only 500 points for a stock and the statistics is poor, we do not test it here. Also for a good statistics we focus on return intervals of a typical threshold, $q = 2$. Similar to the 1-min resolution, most of cases can be well fit by Eq. (5). For instance, with 5-min resolution, the SE hypothesis for 812 of 1000 stocks are not rejected under 1% significance level. In Fig. 5 we show the PDF of γ for $\Delta t = 1$, 5, 10 and 30 minutes. The shape of PDF systematically changes with increasing the sampling interval, the center shifts to right slightly and the width increases, which is consistent with the change of data size. For a lower resolution, we have fewer data points and consequently stronger fluctuations for γ values. Therefore, these curves show the persistence of the scaling for a broad range of sampling intervals.

2.4 Multiscaling

Financial time series are known to show complex behavior and are not of uniscaling nature [74]. The distribution of activity measure such as the intertrade time has multiscaling behavior [75,76]. From the previous sections we also see some weak but systematic tendencies, which indicate possible multiscaling (Fig. 3). Thus, a detailed analysis of the scaling properties of the volatility return intervals is of interest. Moment μ_m, which is defined as

$$\mu_m \equiv \langle (\tau/\langle\tau\rangle)^m \rangle^{1/m}, \tag{9}$$

accumulates the information over the entire data set and therefore provides a good way for testing the deviations from a scaling law. Pure scaling yields that μ_m should be independent on $\langle\tau\rangle$. Here m is the order of moment. Wang et al. studied the moments for 500 component stocks of S&P 500 index and found that μ_m has a certain tendency with $\langle\tau\rangle$, indicating multiscaling in the distribution of τ [60]. As shown in Fig. 6, the four moments of GE have similar tendencies, they increase to a certain value in the small $\langle\tau\rangle$ regime and then start to decrease. To quantify the tendency, Wang et al. suggested to fit the moments with a power-law [60],

$$\mu_m \sim \langle\tau\rangle^{\delta}. \tag{10}$$

If the distribution of return intervals follows a scaling law, the exponent δ should be close to 0. In other words, a significant non-zero δ suggests multiscaling. Here we call δ multiscaling exponent since it characterizes the multiscaling behavior [60]. The power law fit is demonstrated by dashed lines in Fig. 6. For very small and very large values of $\langle\tau\rangle$, Wang et al. identified the discreteness and finite size effects respectively [60], which was also recognized for the general case by Eichner et al. [51]. To avoid these effects, we fit Eq. (10) only in the medium

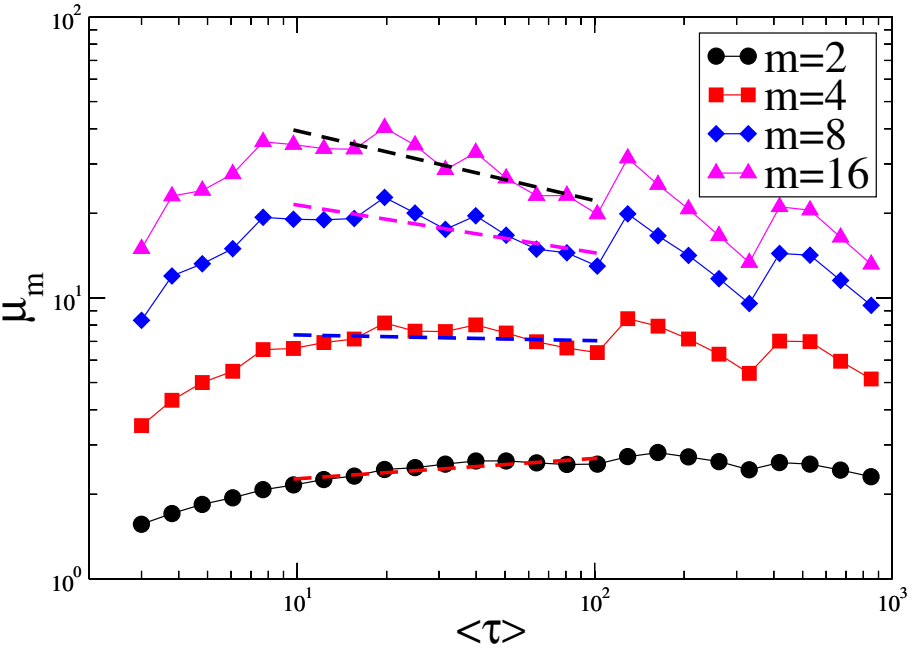

Fig. 6. (Color online) Dependence of moments μ_m on mean interval $\langle\tau\rangle$ for the GE stock. Four orders, $m = 2$, 4, 8 and 16 are showed. Dashed lines are power law fits in the range of $10 < \langle\tau\rangle \leq 100$. Adapted from [61].

range, $10 < \langle\tau\rangle \leq 100$. As shown in Fig. 7, over the 500 component stocks of S&P 500, the average δ systematically changes with m, which supports the existing of multiscaling features in the return interval distribution. Furthermore, we can see that δ are centered around 0 for the surrogate data, suggesting that the multiscaling behavior in the original records is related to the nonlinear correlations in volatility sequence. The surrogate records are generated by the Schreiber method [77,78] where nonlinearities are removed, and the corresponding μ_m is independent with $\langle\tau\rangle$. Ren and Zhou also employed moment analysis on two Chinese indices and confirmed the multiscaling behavior in the return interval distribution [62].

A second way to test the multiscaling is by examining the relation between the correlation exponent γ and threshold q. Wang et al. have shown that γ has a certain dependence on the threshold q for the broad market, especially for small thresholds [61], which is consistent with Fig. 3. A third method for testing is using KS statistics to test compare return interval distributions of two thresholds. If $D > CV$, the null hypothesis that two distributions are same is rejected. For the Japanese market, Jung et al. have shown a good scaling by the KS test [55]. However, for the Chinese market, Ren and Zhou found that the null hypothesis is not rejected only for 12 of 30 liquid stocks. For other 18 stocks,

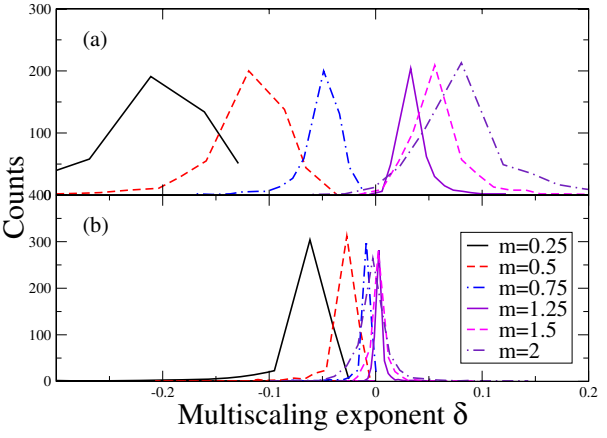

Fig. 7. (Color online) Distribution of multiscaling exponent α for S&P 500 constituents. The exponent α is obtained from the power-law fit for moments in the medium range $10 < \langle\tau\rangle \leq 100$. (a) Histogram of α for the original volatility and (b) for surrogate. The distributions have a systematic shift with m in (a) while all of them almost collapse in (b). This suggests that the multiscaling behavior in the original records dues to the nonlinear correlations in the volatility sequence. Adapted from [60].

the distributions are significantly different for different thresholds therefore they don't obey a single scaling law [62].

2.5 Size Effect

The following question arises, what is the origin for the multiscaling behavior in the return interval distribution? Recently Wang et al. carried out a multi-factor analysis and found similar relations over the factors [61]. Here we focus on the most popular measure, the market capitalization or the size of a stock, which is clearly related to the market activity [76]. Fig. 8 is the scatter plot of the relationship between γ and capitalization for the 1000 stocks. For all the four thresholds, the points are distributed in a wide area, which indicates an insignificant dependence. To better view a possible tendency, we group points according to their logarithmic value of capitalization and plot the average and standard deviation (as the error bar) of γ in each bin, as shown by the triangles in Fig. 8. An increasing trend for most of the range and a drop for very large capitalization is noticed. Interestingly, this behavior is consistent for all four thresholds. Note that the change of average γ is almost in the range of the error bar. Thus, γ systematically depends on the capitalization but the dependence is not strong, which suggests that there is a certain underline nonlinear mechanism and some sort of filtering maybe needed to identify it. Wang et al. also analyzed the dependence on the number of trades, risk and return. They found consistent relation for the risk and return. They also showed that γ is independent on the

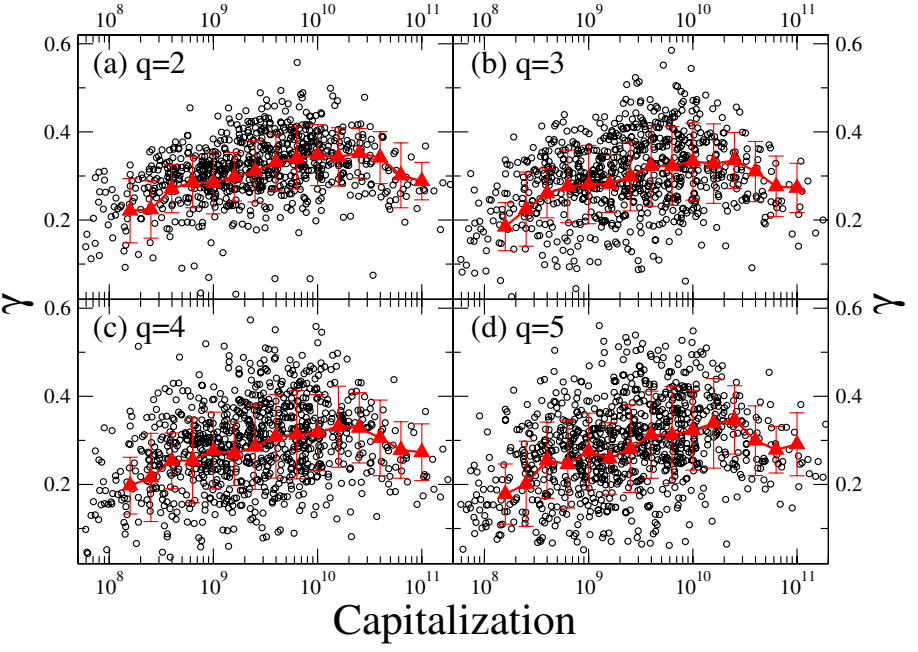

Fig. 8. (Color online) Size effect of correlation exponent γ. Scatter plot of four thresholds, $q = 2$ to 5 are displayed. To better view the tendency, we calculate the average and standard deviation in logarithmic bins of capitalization, as shown by the triangle (average) and error bar (standard deviation). For the four thresholds, average γ increases with the capitalization for most of the range.

number of trades. Similarly, they found a certain dependence on these factors for the multiscaling exponent δ [61].

3 Memory Effects in the Return Interval Sequence

The temporal structure is an essential feature to characterize a time series. It can be examined in different time scales. Here we analyze it in three scales, short, medium and long term.

3.1 Short-Term Memory

The short-term memory can be measured by the conditional PDF, $P(\tau|\tau_0)$, which is the probability of finding a return interval τ immediately after a return interval of size τ_0 [49,50,51,52,53,54]. In records without memory, $P(\tau|\tau_0)$ should be identical to $P(\tau)$ and independent of τ_0. When memory exists, it should depends on the choice of τ_0. Due to the poor statistics for a single value of return interval, a binning of τ_0 is needed. Yamasaki et al. split the entire database into 8 equal-size subsets, Q_1, Q_2, ..., Q_8, with intervals in increasing length [52,53,54].

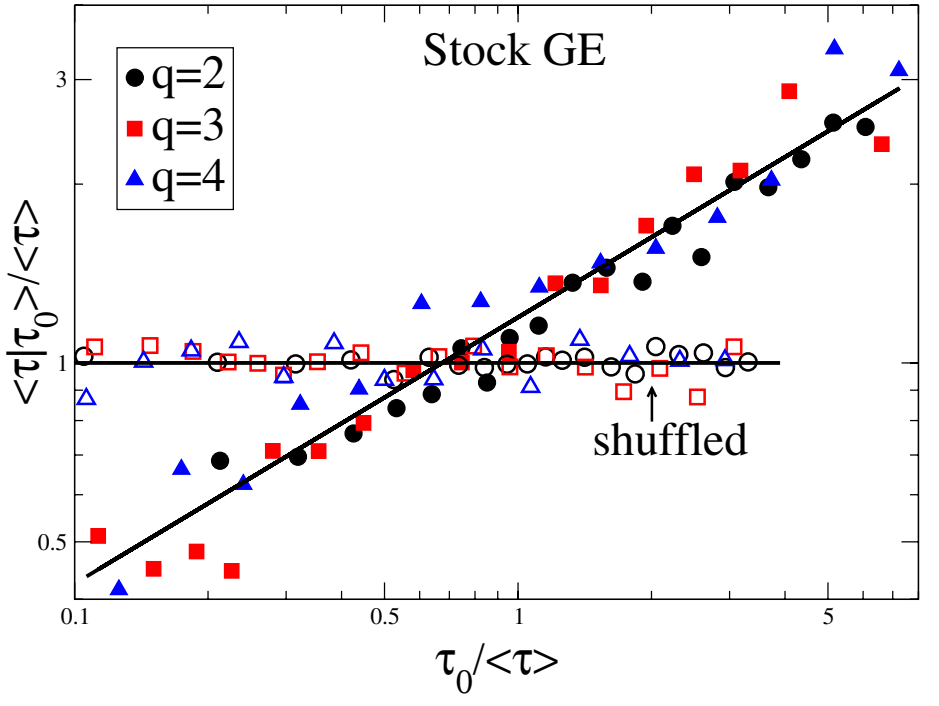

Fig. 9. (Color online) Mean conditional return interval $\langle\tau|\tau_0\rangle/\langle\tau\rangle$ vs $\tau_0/\langle\tau\rangle$ for the GE stock. Symbols are for three different thresholds $q = 2$, 3 and 4. To compare with the real data results (filled symbols), we also plot the corresponding results for shuffled records (open symbols). The distinct difference between the two records implies the memory effect in the original interval sequence. Adapted from [54].

It is found that for τ_0 in Q_1, the probability is higher for small τ, while for τ_0 in Q_8, the probability is higher for large τ. Thus, large (small) τ_0 tends to be followed by large (small) τ ("clustering"), which indicates memory in the sequence. Note that for all thresholds $P(\tau|\tau_0)$ seems to collapse onto a single scaling function for each of the τ_0 subsets, and they can be well fit by a SE function according to Eq. (3). These results are consistent for the US markets, currencies, interest rates and commodities [52,53,54]. Similar results have been found for the Japanese market [55] and Chinese market [56,57].

Further, the short-term memory is also seen clearly in the mean conditional return interval immediately after a given τ_0 subset, $\langle\tau|\tau_0\rangle$, which is the first moment of $P(\tau|\tau_0)$. A power law dependence of $\langle\tau|\tau_0\rangle$ on τ_0 for the GE stock is showed in Fig. 9, as an example. We can see that large (small) τ tend to follow large (small) τ_0, similar to the clustering in $P(\tau|\tau_0)$. Correspondingly, shuffled data (open symbols in Fig. 9) are almost constant as expected, demonstrating that the value of τ is independent of the previous interval τ_0.

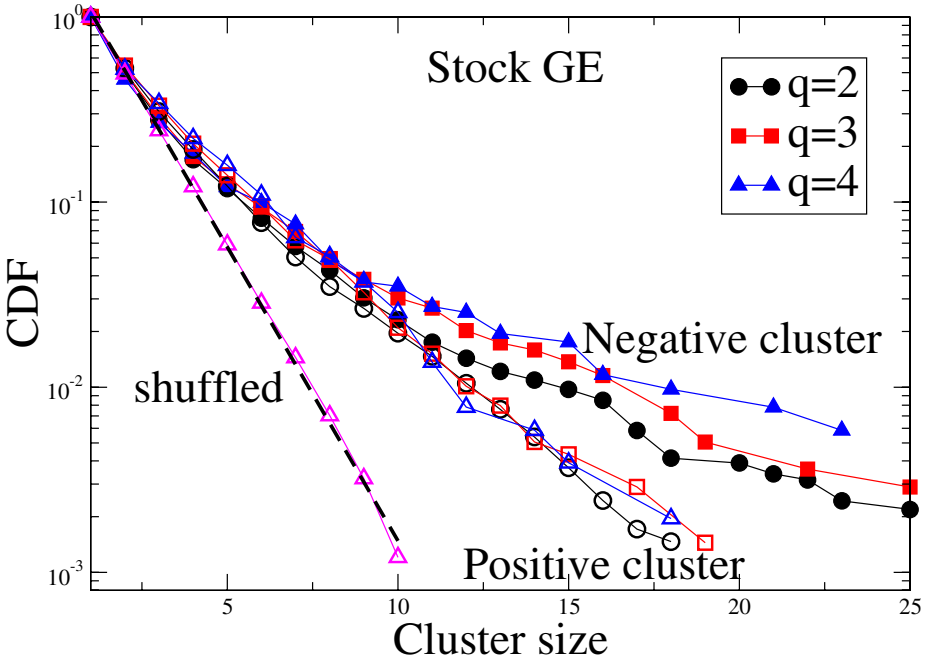

Fig. 10. (Color online) Cumulative distribution of size for return interval clusters. The cluster consists of consecutive return intervals that are all above ("positive cluster", open symbols) or below ("negative cluster", filled symbols) the median of return intervals. For the shuffled records, the distribution follows an exponential function. However, for the original records, their distributions for both positive and negative clusters have much longer tails, suggesting a significant memory in return intervals. Adapted from [54].

3.2 Clustering

Clustering phenomena are displayed by $P(\tau|\tau_0)$ and $\langle\tau|\tau_0\rangle$, indicating the memory in the return intervals. However, both functions measure the intervals that immediately follow an interval τ_0. In order to investigate longer clustering in a straighter way, we analyze "clusters" of return intervals, which are composed by successive intervals with similar size [53,54,55,56,58]. To obtain good statistics we divide the sequence of return intervals into two bins, separated by the median of the entire database. We denote intervals that are above the median by sign "+", and the ones below the median by "–". Accordingly, consecutive "+" or "–" intervals form a positive or negative cluster.

The distribution of cluster sizes n reveal the memory information in the sequence. Fig. 10 shows the cumulative distribution of the cluster size for the GE stock. Both positive and negative clusters have quite long tails, compared to that for the shuffled records which follows an exponential function and shows a much

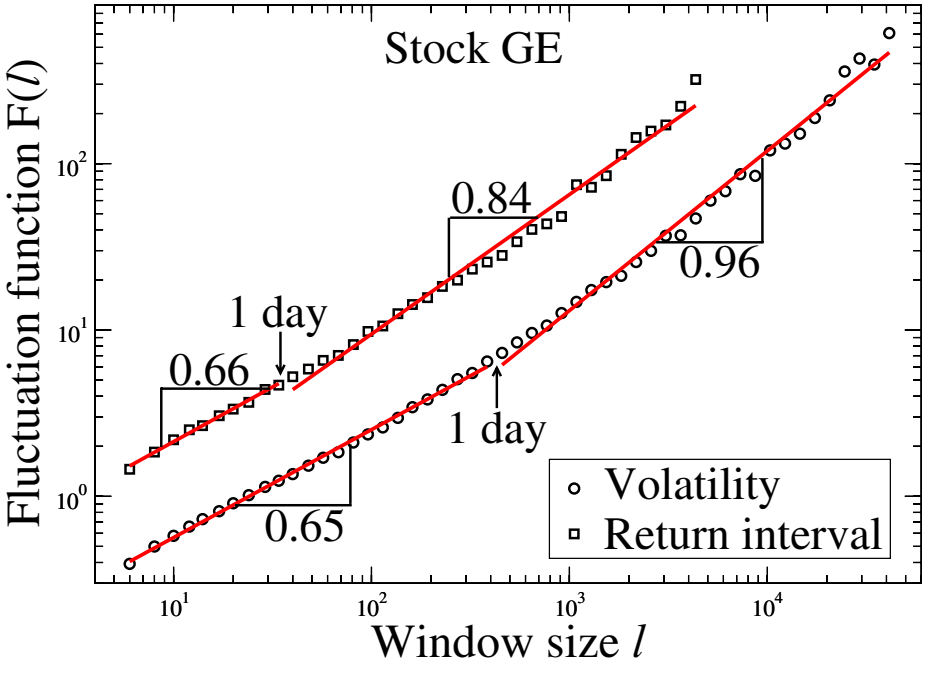

Fig. 11. (Color online) Detrended fluctuation analysis (DFA) on the volatility and return interval ($q = 2$) for the GE stock. Two curves are similar and their crossovers are around 1 trading day. Solid lines are for power law fits on the two regimes. For short scale, two α (slopes in the plot) are almost same. For long scale, two α are different but they are strongly related.

faster decay. For the positive clusters, the distribution still has good statistics even for size $n = 18$, while the negative clusters extend to $n = 25$. Thus, the memory effects persist for quite long times (e.g., the average return interval for GE with threshold $q = 2$ is about 9 minutes, so there are still some clusters corresponding to even 200 minutes in the time scale). Note that the distribution of positive clusters is very similar for different thresholds $q = 2, 3, 4$, while the negative clusters show the same effect only for $n \leq 10$. Similar clustering has been found also in earthquake and climate data [50,79].

3.3 Long-Term Correlations

The volatility is known to have long-term correlations [31], thus an examination of long-term correlations in the return interval is needed. We apply the Detrended Fluctuation Analysis (DFA) method [80,81,82] to the volatility and their return interval sequence. Without loss of generality, we investigate the return interval for a typical threshold $q = 2$. After removing trends, DFA computes the

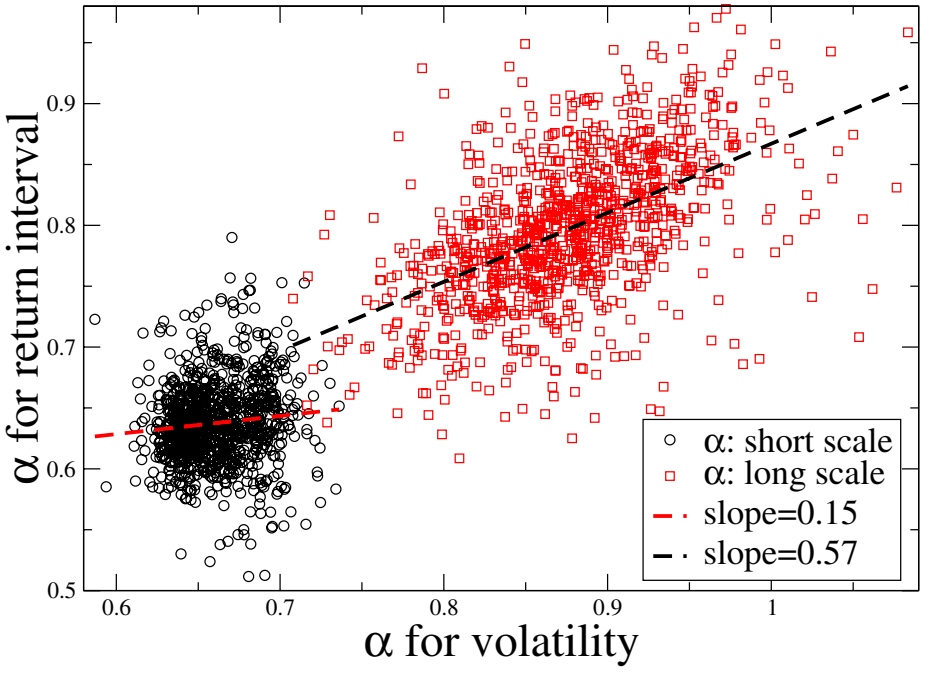

Fig. 12. (Color online) Dependence of long-term correlations in the volatility and the return interval ($q = 2$) sequence. The results for two scale regimes are showed. As indicated by the two linear fits on the symbols (dashed lines), the dependence is not strong for the short scale but it is significant for the long scale. The weak relation for short scale is related to the small range of their α.

root-mean-square fluctuation $F(\ell)$ of a time series within windows of ℓ points, and determines the exponent α from the scaling function,

$$F(\ell) \sim \ell^{\alpha}. \tag{11}$$

The correlation in the time series is characterized by the exponent $\alpha \in (0, 1)$. If $\alpha > 0.5$, the records has positive correlations If $\alpha = 0.5$, it has no correlation (white noise). If $\alpha < 0.5$, it has negative correlations.

Similar to the volatility [31], there is a crossover in the DFA curve for return interval thus the entire regime can be split into two sub-regimes $\ell < \ell^*$ and $\ell > \ell^*$ (ℓ^* is chose for that the corresponding time spanned is 390 minutes or 1 trading day) [31,53]. As an example, we show DFA curves for volatility and return interval ($q = 2$) of the GE stock in Fig. 11. We see that the corresponding values for α are distinctly different in the two regimes. However, both α are significantly larger than 0.5, suggesting long-term correlations in return intervals. In the short scale regime ($\ell < \ell^*$), we find $\alpha = 0.64 \pm 0.04$ for the return interval of the 1000 stocks, while $\alpha = 0.66 \pm 0.02$ for the volatility. The two cases are almost the same. In the long scale regime ($\ell > \ell^*$), we find $\alpha = 0.80 \pm 0.06$ for

the return interval and $\alpha = 0.88 \pm 0.06$ for the volatility. and the discrepancy is slightly larger but in the range of the error bars. Here error bar refers to the standard deviation of the 1000 stocks. Such behavior suggests a common origin for the strong persistence of correlations in both volatility and return interval records, and in fact the clustering in return intervals is related to the known effect of volatility clustering [19]. To further examine the relation between two types of α, we draw the scatter plot for the dependence of two α in two regimes respectively, as shown in Fig. 12. We can see a significant dependence for α in the long scale. However, α for the short scale are crowded together so that there is no strong tendency.

4 Models

To further understand the financial fluctuations, Vodenska-Chitkushev et al. simulated models for the volatility series and tested the corresponding return intervals. Two popular long-term memory models, FIGARCH [83] and fractional Brownian motion (fBm) [84] are examined (see Ref [58] and references therein).

4.1 FIGARCH

Fractional integrated generalized autoregressive conditional heteroscedasticity (FIGARCH) [83] is a popular model for the return simulation. In this model the return r_t can be generated by the following process,

$$r_t = \mu + a(L) \cdot \epsilon_t. \tag{12}$$

Here μ is the mean value of return, L is the lag operator, $a(L)$ is the coefficient from the autoregressive moving average (ARMA) procedure, and ϵ_t is the disturbance term,

$$\epsilon_t \equiv z_t \cdot \sigma_t. \tag{13}$$

z_t is an *i.i.d.* process with zero mean and unit variance, and the conditional variance σ_t^2 is determined by the following process,

$$\sigma_t^2 = \sigma^2 + \lambda(L) \cdot (\epsilon_t^2 - \sigma^2). \tag{14}$$

Here σ^2 is the unconditional variance of ϵ_t, and $\lambda(L)$ is from ARCH and GARCH coefficients which follows $\lambda(L) \sim (1-L)^d$. $d \in (0,1)$ is the fractional differencing parameter and $\lambda(L)$ can be expanded into an infinite polynomial of L. FIGARCH process can captures the long-term dependence in volatilities, which is connected to the parameter d. When d increases, the long-term memory will gradually vanish.

After extracting parameters from the S&P 500 index data, we simulate returns from which volatilities are derived and analyze their return intervals properties [58]. First, we test the scaling of return intervals distribution, as shown in Fig. 13. There are significant deviations from the scaling for both small and large intervals. This result manifests that FIGARCH does not show good scaling in

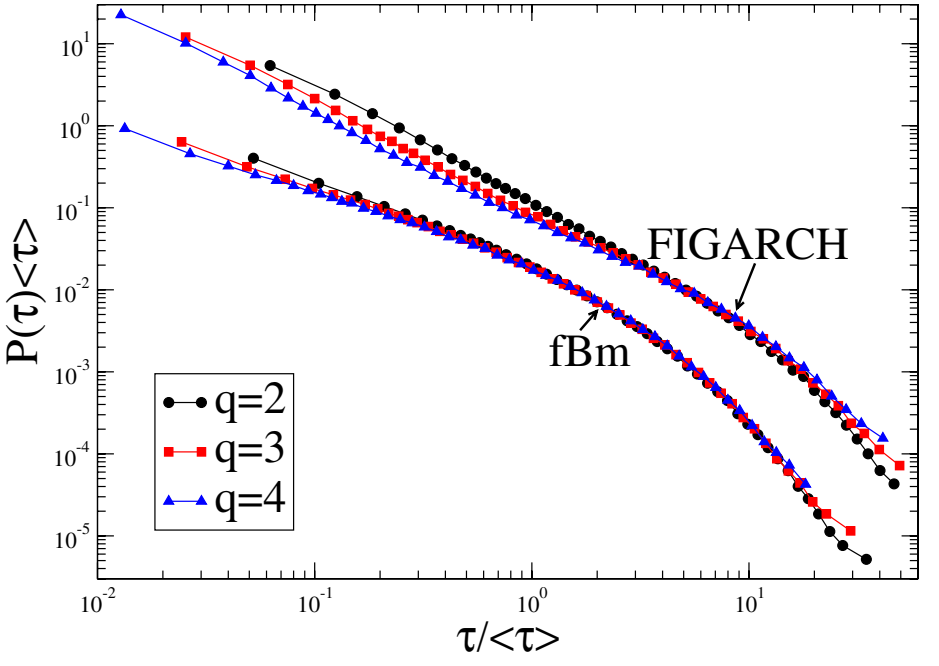

Fig. 13. (Color online) Scaling in the distribution of return intervals for two models, FIGARCH and fBm. Curves for fBm are vertically shifted down for better visibility. For FIGARCH, the scaled PDF, $P(\tau) \cdot \langle\tau\rangle$, does not collapse onto a single curve, especially for small and large scaled interval $\tau/\langle\tau\rangle$, which suggests no good scaling. For fBm, the three scaled PDFs collapse for most of range (the small deviations at very small or very large scaled intervals correspond to discreteness and finite size effects respectively). This indicates a good scaling in the distribution for the fBm model.

the return interval distribution. Further, we examine the cluster size distribution, which is demonstrated in Fig. 14. We can see that FIGARCH captures the memory effects for both positive and negative clusters. Their effects are slightly stronger than the empirical memory.

4.2 Fractional Brownian Motion

Fractional Brownian motion (fBm) [84] is a generalization of Brownian motion. The only difference from a regular Brownian motion is that the increments of fBm are correlated. The long-range dependence of the increments can be characterized by the Hurst parameter $H \in (0, 1)$, which is the only parameter to index a fBm process $B_H(t)$. Note that $B_H(t)$ reduces to a regular Brownian motion when $H = 1/2$, while $H > 1/2$ ($H < 1/2$) corresponds to positive (negative) correlation. An important feature of fBm is the scale invariance,

$$B_H(c \cdot t) = c^H \cdot B_H(t) \tag{15}$$

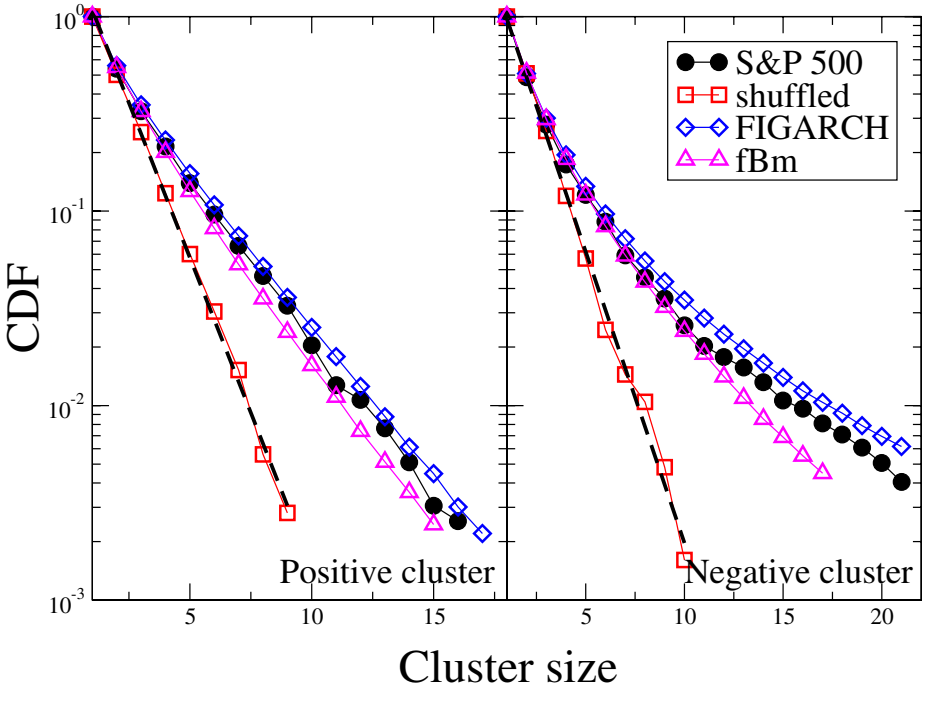

Fig. 14. (Color online) Cluster size distribution for the FIGARCH and fBm models. The output of two models are very close to that of S&P 500 index and significantly away for the shuffled data, which suggests that the memory in the empirical data can be repeated by both FIGARCH and fBm. The figure shows that FIGARCH slightly overestimates the memory while fBm slightly underestimates it.

for all $c > 0$. Since the return only has short-term correlations while the volatility has long-term correlations, we simulate the return by

$$r_t = e^{B_H(t+1)-B_H(t)} \cdot \eta_t \tag{16}$$

where η_t is an i.i.d. process with zero mean and unite variance.

We simulate return intervals with fBm process and calculated their PDF and distributions of cluster size [85]. PDF of return intervals is showed in Fig. 13, which has a well-approximated scaling. In Fig. 14, the cluster size distributions of fBm process is quite close to the empirical data. The two curves are only slightly smaller for both positive and negative cluster.

5 Conclusions

We analyzed the properties of the return intervals for the 1000 most traded stocks in the US markets, as well as reviewed recent studies on return interval analysis.

We showed that there is a good scaling in the return interval distribution and the scaling function can be approximated by a stretched exponential with correlation exponent around 0.4. Importantly, the behavior is universal for a wide range of thresholds, many financial assets and a broad scale of sampling intervals. On the other hand, we found that the power law distribution is not ruled out for the distribution tail, especial for return intervals of large thresholds. The tail exponent systematically shifts from 2 to 1 for the threshold from 2 to 5 standard deviations. We also employed moment analysis to examine the existence of multiscaling in the distribution. Further we connected this behavior to the company size and found a weak dependence.

Further more we analyzed memory effects in various time scales, from the immediate conditional PDF and mean interval, clusters classified by the median of return intervals to long-term correlations. We showed memories in all of these investigations. Interestingly, the long-term correlations in return intervals are strongly related to the long-term correlations in the volatility sequence.

Moreover, we tested two popular long-term memory models, FIGARCH and fBm. Only fBm shows a good scaling in the distribution. However, both models catch the memory effect. FIGARCH slightly overestimates the effect while fBm slightly underestimate it.

Acknowledgments

We thank S.-J. Shieh, X. Gabaix, P. Gopikrishnan, V. Plerou, B. Rosenow, J. Nagler, F. Pammolli and especially A. Bunde, L. Muchnik, P. Weber, W.-S. Jung and I. Vodenska-Chitkushev for collaboration on many aspects of this research, and the NSF and Merck Foundation for financial support.

References

1. Pareto, V.: Cours d'Economie Politique, Lausanne and Paris (1897)
2. Bachelier, L.: Théorie de la spéculation [Ph.D. thesis in mathematics]. Annales Scientifiques de l'Ecole Normale Supérieure III-17, 21 (1900); translated and Reprinted in, Cootner, P. (ed.). The Random Character of Stock Market Prices, p. 17. MIT Press, Cambridge (1967)
3. Lévy, P.: Théorie de l'Addition des Variables Aléatoires, Gauthier-Villars, Paris (1937)
4. Fama, E.F.: J. Business 36, 420 (1963)
5. Officer, R.R.: J. Amer. Statistical Assoc. 67, 807 (1972)
6. Clark, P.K.: Econometrica 41, 135 (1973)
7. Wood, R.A., McInish, T.H., Ord, J.K.: J. Finance 40, 723 (1985)
8. Harris, L.: J. Financ. Econ. 16, 99 (1986)
9. Admati, A., Pfleiderer, P.: Rev. Financ. Stud. 1, 3 (1988)
10. Schwert, G.W.: J. Finance 44, 1115 (1989); Chan, K., Chan, K.C., Karolyi, G.A.: Rev. Financ. Stud. 4, 657 (1991); Bollerslev, T., Chou, R.Y., Kroner, K.F.: J. Econometr. 52, 5 (1992); Gallant, A.R., Rossi, P.E., Tauchen, G.: Rev. Financ. Stud. 5, 199 (1992); Le Baron, B.: J. Business 65, 199 (1992)

11. Ding, Z., Granger, C.W.J., Engle, R.F.: J. Empirical Finance 1, 83 (1993)
12. Dacorogna, M.M., Muller, U.A., Nagler, R.J., Olsen, R.B., Pictet, O.V.: J. Int. Money Finance 12, 413 (1993)
13. Loretan, M., Phillips, P.C.B.: J. Empirical Finance 1, 211 (1994)
14. Pagan, A.: J. Empirical Finance 3, 15 (1996)
15. Mantegna, R.N., Stanley, H.E.: Nature 383, 587 (1996)
16. Cizeau, P., Liu, Y., Meyer, M., Peng, C.-K., Stanley, H.E.: Physica A 245, 441 (1997)
17. Cont, R.: Ph.D. thesis, Universite de Paris XI (1998) (unpublished); see also e-print cond-mat/9705075
18. Pasquini, M., Serva, M.: Econ. Lett. 65, 275 (1999)
19. Lux, T., Marchesi, M.: Int. J. Theor. Appl. Finance 3, 675 (2000); Giardina, I., Bouchaud, J.-P.: Physica A 299, 28 (2001); Lux, T., Ausloos, M.: In: Bunde, A., Kropp, J., Schellnhuber, H.J. (eds.) The Science of Disasters: Climate Disruptions, Heart Attacks, and Market Crashes, p. 373. Springer, Berlin (2002)
20. Rosenow, B.: Int. J. Mod. Phys. C 13, 419 (2002)
21. Gabaix, X., Gopikrishnan, P., Plerou, V., Stanley, H.E.: Nature 423, 267 (2003); Gabaix, X., Gopikrishnan, P., Plerou, V., Stanley, H.E.: Quart. J. Econ. 121, 461 (2006)
22. Farmer, J.D., Gillemot, L., Lillo, F., Mike, S., Sen, A.: Quant. Finance 4, 383 (2004); Farmer, J.D., Lillo, F.: ibid 4, C8, (2004); Plerou, V., Gopikrishnan, P., Gabaix, X., Stanley, H.E.: ibid 4, C11 (2004)
23. Lillo, F., Farmer, J.D., Mantegna, R.N.: Nature 421, 129 (2003)
24. Weber, P., Wang, F., Vodenska-Chitkushev, I., Havlin, S., Stanley, H.E.: Phys. Rev. E 76, 016109 (2007)
25. Eisler, Z., Bartos, I., Kertész, J.: Adv. Phys. 57, 89 (2008)
26. Jung, W.-S., Kwon, O., Wang, F., Kaizoji, T., Moon, H.-T., Stanley, H.E.: Physica A 387, 537 (2008)
27. Lux, T.: Appl. Finan. Econ. 6, 463 (1996)
28. Gopikrishnan, P., Meyer, M., Amaral, L.A.N., Stanley, H.E.: Eur. Phys. J. B 3, 139 (1998)
29. Muller, U.A., Dacorogna, M.M., Pictet, O.V.: Heavy Tails in High-Frequency Financial Data. In: Adler, R.J., Feldman, R.E., Taqqu, M.S. (eds.) A Practical Guide to Heavy Tails, p. 83. Birkhäuser Publishers, Basel (1998)
30. Plerou, V., Gopikrishnan, P., Amaral, L.A.N., Meyer, M., Stanley, H.E.: Phys. Rev. E 60, 6519 (1999); Plerou, V., Gopikrishnan, P., Amaral, L.A.N., Gabaix, X., Stanley, H.E.: ibid 62, 3023 (2000); Gopikrishnan, P., Plerou, V., Gabaix, X., Stanley, H.E.: ibid 62, 4493 (2000)
31. Liu, Y., Gopikrishnan, P., Cizeau, P., Meyer, M., Peng, C.-K., Stanley, H.E.: Phys. Rev. E 60, 1390, (1999); Plerou, V., Gopikrishnan, P., Gabaix, X., Amaral, L.A.N., Stanley, H.E.: Quant. Finance 1, 262, (2001); Plerou, V., Gopikrishnan, P., Stanley, H.E.: Phys. Rev. E 71, 046131 (2005); for application to heartbeat intervals see, Ashkenazy, Y., Ivanov, P.C., Havlin, S., Peng, C.-K., Goldberger, A.L., Stanley, H.E.: Phys. Rev. Lett. 86, 1900 (2001)
32. Plerou, V., Stanley, H.E.: Phys. Rev. E 76, 046109 (2007)
33. Clauset, A., Shalizi, C.R., Newman, M.E.J.: `http://arxiv.org/abs/0706.1062v1`
34. Mantegna, R., Stanley, H.E.: Introduction to Econophysics: Correlations and Complexity in Finance. Cambridge Univ. Press, Cambridge (2000)
35. Mandelbrot, B.B.: J. Business 36, 394 (1963)
36. Bunde, A., Havlin, S. (eds.): Fractals in Science. Springer, Heidelberg (1994)

37. Mantegna, R.N., Stanley, H.E.: Nature 376, 46 (1995)
38. Stanley, H.E.: Introduction to Phase Transitions and Critical Phenomena. Oxford University Press, Oxford (1971)
39. Stanley, H.E.: Rev. Mod. Phys. 71, 358 (1999)
40. Peng, C.K., Buldyrev, S., Goldberger, A., Havlin, S., Sciortino, F., Simons, M., Stanley, H.E.: Nature 356, 168 (1992); Buldyrev, S.V., Goldberger, A.L., Havlin, S., Peng, C.-K., Stanley, H.E., Stanley, M.H.R., Simons, M.: Biophys. J. 65, 2673 (1993); Buldyrev, S.V., Goldberger, A.L., Havlin, S., Peng, C.-K., Simons, M., Stanley, H.E.: Phys. Rev. E 47, 4514 (1993); Mantegna, R.N., Buldyrev, S.V., Goldberger, A.L., Havlin, S., Peng, C.-K., Simons, M., Stanley, H.E.: Phys. Rev. E 52, 2939 (1995)
41. Suki, B., Barabási, A.-L., Hantos, Z., Peták, F., Stanley, H.E.: Nature 368, 615 (1994)
42. Peng, C.K., Mietus, J., Hausdorff, J., Havlin, S., Stanley, H.E., Goldberger, A.L.: Phys. Rev. Lett. 70, 1343 (1993)
43. Makse, H.A., Havlin, S., Stanley, H.E.: Nature 377, 608 (1995); Makse, H.A., Andrade, J.S., Batty, M., Havlin, S., Stanley, H.E.: Phys. Rev. E 58, 7054 (1998)
44. Plerou, V., Amaral, L.A.N., Gopikrishnan, P., Meyer, M., Stanley, H.E.: Nature 400, 433 (1999)
45. Keitt, T.H., Stanley, H.E.: Nature 393, 257 (1998); Keitt, T.H., Amaral, L.A.N., Buldyrev, S.V., Stanley, H.E.: Scaling in the Growth of Geographically Subdivided Populations: Scale-Invariant Patterns from a Continent-Wide Biological Survey. Focus issue: The Biosphere as a Complex Adaptive System, Phil. Trans. Royal Soc. B: Biological Sciences 357, 627 (2002)
46. Gutenberg, B., Richter, C.F.: Seismicity of the Earth and Associated Phenomenon, 2nd edn. Princeton University Press, Princeton (1954)
47. Turcotte, D.L.: Fractals and Chaos in Geology and Geophysics. Cambridge University Press, Cambridge (1992)
48. Bunde, A., Eichner, J.F., Havlin, S., Kantelhardt, J.W.: Physica A, 342, 308 (2004)
49. Bunde, A., Eichner, J.F., Kantelhardt, J.W., Havlin, S.: Phys. Rev. Lett. 94, 048701 (2005)
50. Livina, V.N., Havlin, S., Bunde, A.: Phys. Rev. Lett. 95, 208501 (2005)
51. Eichner, J.F., Kantelhardt, J.W., Bunde, A., Havlin, S.: Phys. Rev. E 75, 011128 (2007)
52. Yamasaki, K., Muchnik, L., Havlin, S., Bunde, A., Stanley, H.E.: Proc. Natl. Acad. Sci. U.S.A. 102, 9424, (2005); Yamasaki, K., Muchnik, L., Havlin, S., Bunde, A., Stanley, H.E.: In: Takayasu, H. (ed.) Proceedings of the Third Nikkei Econophysics Research Workshop and Symposium, The Fruits of Econophysics, Tokyo, p. 43. Springer, Berlin (2005)
53. Wang, F., Yamasaki, K., Havlin, S., Stanley, H.E.: Phys. Rev. E 73, 026117 (2006)
54. Wang, F., Weber, P., Yamasaki, K., Havlin, S., Stanley, H.E.: Eur. Phys. J. B 55, 123 (2007)
55. Jung, W.-S., Wang, F.Z., Havlin, S., Kaizoji, T., Moon, H.-T., Stanley, H.E.: Eur. Phys. J. B 62, 113 (2008)
56. Qiu, T., Guo, L., Chen, G.: Physica A 387, 6812 (2008)
57. Ren, F., Guo, L., Zhou, W.-X.: http://arxiv.org/abs/0807.1818v1
58. Vodenska-Chitkushev, I., Wang, F.Z., Weber, P., Yamasaki, K., Havlin, S., Stanley, H.E.: Eur. Phys. J. B 61, 217 (2008)
59. Bogachev, M.I., Eichner, J.F., Bunde, A.: Phys. Rev. Lett. 99, 240601 (2007)
60. Wang, F., Yamasaki, K., Havlin, S., Stanley, H.E.: Phys. Rev. E 77, 016109 (2008)

61. Wang, F., Yamasaki, K., Havlin, S., Stanley, H.E.: http://arxiv.org/abs/0808.3200v1
62. Ren, F., Zhou, W.-X.: http://arxiv.org/abs/0809.0250v1
63. Bogachev, M.I., Bunde, A.: Phys. Rev. E 78, 036114 (2008)
64. Black, F., Scholes, M.: J. Polit. Econ. 81, 637 (1973)
65. Cox, J.C., Ross, S.A.: J. Financ. Econ. 3, 145 (1976); Cox, J.C., Ross, S.A., Rubinstein, M.: J. Financ. Econ. 7, 229 (1979)
66. Bouchaud, J.-P., Potters, M.: Theory of Financial Risk and Derivative Pricing: From Statistical Physics to Risk Management. Cambridge Univ. Press, Cambridge (2003)
67. Johnson, N.F., Jefferies, P., Hui, P.M.: Financial Market Complexity. Oxford Univ. Press, New York (2003)
68. Altmann, E.G., Kantz, H.: Phys. Rev. E 71, 056106 (2005)
69. Stephens, M.A.: J. Am. Stat. Assoc. 69, 730 (1974)
70. Engle, R., Russel, J.: Econometrica 66, 1127 (1998)
71. To avoid the discreteness for small τ (Ref [51] suggested a power law function for this range) and large fluctuations for very large τ, we choose the range of $0.01 \leq CDF \leq 0.50$ to perform the stretched exponential fit
72. It sounds that the ratio between two a significantly deviates from 1. However, it is not that huge if we test the sensitivity on γ for Eq. (4). For instance, when γ changes from 0.30 to 0.31, the value a from Eq. (4) increases more than 30% with a constant $\langle\tau\rangle$
73. Hill, B.M.: Ann. Stat. 3, 1163 (1975)
74. Di Matteo, T.: Quant. Finan. 7, 21 (2007)
75. Ivanov, P.C., Yuen, A., Podobnik, B., Lee, Y.: Phys. Rev. E 69, 056107 (2004)
76. Eisler, Z., Kertész, J.: Phys. Rev. E 73, 046109 (2006); Eisler, Z., Kertész, J.: Eur. Phys. J. B 51, 145 (2006)
77. Schreiber, T., Schmitz, A.: Phys. Rev. Lett. 77, 635 (1996); Schreiber, T., Schmitz, A.: Physica D 142, 346 (2000)
78. Makse, H.A., Havlin, S., Schwartz, M., Stanley, H.E.: Phys. Rev. E 53, 5445 (1996)
79. Eichner, J.F., Kantelhardt, J.W., Bunde, A., Havlin, S.: Phys. Rev. E 73, 016130 (2006)
80. Peng, C.-K., Buldyrev, S.V., Havlin, S., Simons, M., Stanley, H.E., Goldberger, A.L.: Phys. Rev. E 49, 1685 (1994); Peng, C.-K., Havlin, S., Stanley, H.E., Goldberger, A.L.: Chaos 5, 82 (1995)
81. Hu, K., Ivanov, P.C., Chen, Z., Carpena, P., Stanley, H.E.: Phys. Rev. E 64, 011114 (2001); Chen, Z., Ivanov, P.C., Hu, K., Stanley, H.E.: ibid 65, 041107 (2002); Xu, L., Ivanov, P.C., Hu, K., Chen, Z., Carbone, A., Stanley, H.E.: ibid 71, 051101 (2005); Chen, Z., Hu, K., Carpena, P., Bernaola-Galvan, P., Stanley, H.E., Ivanov, P.C.: ibid 71, 011104 (2005); Kantelhardt, J.W., Zschiegner, S., Koscielny-Bunde, E., Havlin, S., Bunde, A., Stanley, H.E.: Physica A 316, 87 (2002)
82. Bunde, A., Havlin, S., Kantelhardt, J.W., Penzel, T., Peter, J.-H., Voigt, K.: Phys. Rev. Lett. 85, 3736 (2000)
83. Baillie, R.T., Bollerslev, T., Mikkelsen, H.O.: J. Econometrics 74, 3 (1996)
84. Mandelbrot, B.B., Van Ness, J.W.: SIAM rev. 10, 442 (1968)
85. To simplify the simulation and without loss of generality, we neglect the crossover in the DFA curve and obtain H = 0.86 for the S&P 500 index